

## Supplementary Information

# Point-of-need diagnostics in a post-Covid world: An opportunity for paper-based microfluidics to serve during syndemics

Maria-Nefeli Tsaloglou, Dionysios C. Christodouleas, Jonathan Milette, Kendall Milkey, Isabelle C. Romine, Judy Im, Duraipandian Thava Selvam, Hadley D. Sikes, and George M. Whitesides

### Table of Contents

1. Development of Paper-based Tests for Detection of Brucellosis during a US DoD project...	2
1.1. Introduction.....	2
1.1.1. Underlying assay chemistries .....	2
1.1.2. Key prior published work on paper-based devices by us & others .....	3
1.2. Experimental Design .....	3
1.2.1. Proof-of-concept device of indirect immunoassay for brucellosis using gold nanoparticles as a detection method .....	3
1.2.2. Proof-of-concept device of indirect immunoassay for brucellosis using polymerization-based amplification (PBA) as a detection method .....	7
1.3. Results.....	7
1.3.1. Proof-of-concept studies of indirect immunoassays for the detection of brucellosis	7
2. Proof-of-concept studies of indirect, multiplexed immunoassays for the detection of HIV and other STDs .....	9
2.1. Experimental Design .....	9
2.1.1. Results.....	10
3. References.....	12

# 1. Development of Paper-based Tests for Detection of Brucellosis during a US DoD project

## 1.1. Introduction

### 1.1.1. Underlying assay chemistries

The principle of an indirect immunoassay using gold nanoparticles for visual readout is shown in Figure SI1.

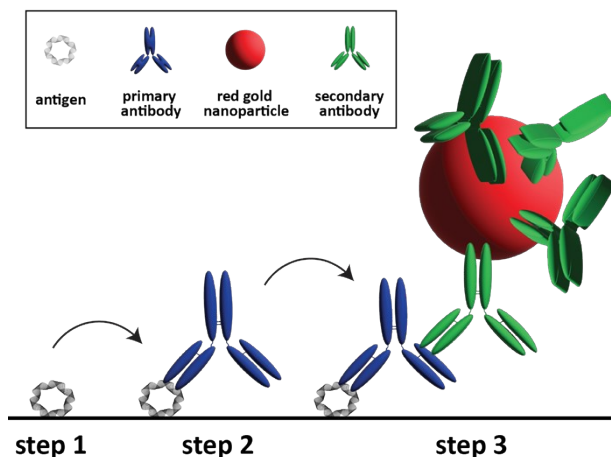
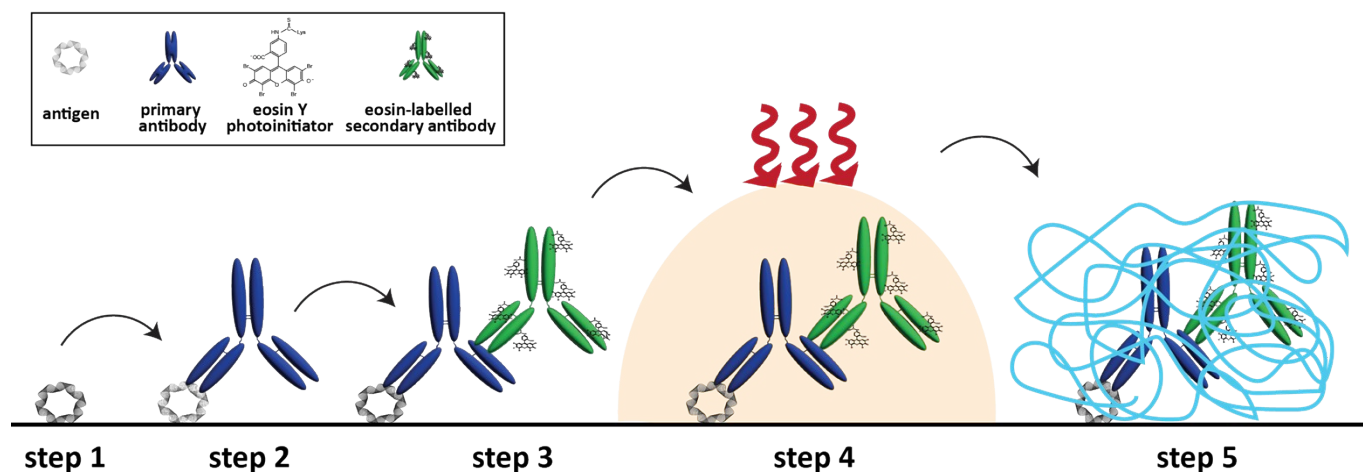


Figure SI1. Illustration of an indirect immunoassay using gold nanoparticles for visual readout. In step 1, an antigen specific to the target of interest is immobilized on a cellulosic surface. In step 2, a primary anti-target antibody binds to the antigen, if present in the sample tested. In step 3, the surface is washed with solution of gold nanoparticles, which have been conjugated to secondary antibodies. In a positive sample, the antigen-primary antibody-secondary antibody sandwich forms, leading to visible agglutination of gold nanoparticles. Diagram is not to scale.

This type of assay is similar the familiar pregnancy test and is often used in paper-based devices. The unique nuance of pregnancy tests is that (although formally not a direct assay), it uses a sandwich arrangement with one capture and one label antibody. Indirect immune assays can be combined with polymerization-based amplification (PBA), which relies on the fact that a single radical causes many chain growth events and uses very low-cost reagents (Figure SI2). PBA shows an extremely rapid assay time (<35 seconds) and can be coupled with nanomolar sensitivity reported in other immunoassays<sup>9</sup>, including for SARS-CoV-2.<sup>10</sup>



**Figure SI2.** Illustration of polymerization-based amplification (PBA) on a porous substrate coupled with an indirect immunoassay. In step 1, an antigen specific to the target of interest is immobilized on a cellulosic surface, which has been aldehyde-functionalized. In step 2, a primary anti-target antibody binds to the antigen, if present in the sample tested. In step 3, a solution containing the secondary antibody conjugated to eosin photo-initiator is used to wash the cellulosic surface. In a positive sample, the antigen-primary antibody-secondary antibody sandwich forms. A monomer solution is added and exposed to UV light (530 nm at 30 mW/cm<sup>2</sup>) in step 4. In step 5, a basic solution (0.5 mM NaOH) is used to either wash away unreacted monomer or visualize the formed hydrogel.

### 1.1.2. Key prior published work on paper-based devices by us & others

In the Whitesides lab, we previously developed a low-cost, paper-based serological test for C-reactive protein in human blood serum.<sup>11</sup> This was an example of implementing enzyme-linked immunosorbent assay (ELISA) on a low-cost device. The PBA method was pioneered at the Sikes lab at MIT, and has been demonstrated on paper-based analytical devices by us and others.<sup>12–15</sup>

For detection of nucleic acids on paper-based devices, we demonstrated an electrochemical molecular test for the detection of DNA from *Mycobacterium* spp.<sup>16</sup> and a paper machine for fluorescence-based, molecular detection of E.coli.<sup>17</sup>

## 1.2. Experimental Design

### 1.2.1. Proof-of-concept device of indirect immunoassay for brucellosis using gold nanoparticles as a detection method

We developed a batch mode manufacturing line for the fabrication of paper-based devices. Each batch yields 32 individual devices, which are complete with spotted reagents. Each batch uses the maximum size of Whatman® Chromatography A paper (20 cm x 20 cm). Layers of adhesive patterned tape and paper are assembled on a custom-made, 3D printed base with integrated pillars for alignment and accurate placement of each layer. To achieve the requirements of 100 tests per batch, we are using three bases at the same time. We also conjugated gold nanoparticles (40 nm, 15 OD, Gold-in-a-Box™) with a monoclonal, mouse anti-bovine IgM secondary antibody (Sigma Aldrich, MA1-90180).

Each device has 14 separate layers (see Figure SI3, overleaf). We have grouped the layers in six separate groups to facilitate manufacturing (see Figure SI4):

1. Group A
  - a. Layer 1: top
  - b. Layer 2: entry
2. Group B
  - a. Layer 3: storage and splitting
3. Group C
  - a. Layer 4: valve and junction
4. Group D
  - a. Layer 6: junction 2
  - b. Layer 7: splitting 1
  - c. Layer 8: splitting 2
  - d. Layer 9: splitting 3
5. Group E
  - a. Layer 10: sensing
  - b. Layer 11: dock
6. Group F
  - a. Layer 12: washing and blotting

Design	Layer	Function
	1. Top	<ul style="list-style-type: none"> <li>Creates 3 cavities (1 sample (S) &amp; 2 buffers (B))</li> <li>Incorporates a blood separation membrane</li> </ul>
	2. Entry	<ul style="list-style-type: none"> <li>Serves as entry point for the sample and the buffer channels</li> </ul>
	3. Splitting & storage	<ul style="list-style-type: none"> <li>Splits the sample evenly</li> <li>Stores the reporter antibodies conjugated to gold nanoparticles in the buffer channel (red)</li> </ul>
	4. Valve	<ul style="list-style-type: none"> <li>L4: Incorporates a valve into the buffer channels</li> </ul>
	5. Junction 1	<ul style="list-style-type: none"> <li>L5: Facilitates fluid flow</li> </ul>
	6. Junction 2	<ul style="list-style-type: none"> <li>Connects the buffer channels to the sample channels</li> </ul>
	7. Splitting 1	<ul style="list-style-type: none"> <li>Facilitates fluids flow &amp; stores buffer salt</li> </ul>
	8. Splitting 2	<ul style="list-style-type: none"> <li>Splits the fluids evenly &amp; stores buffer salt</li> </ul>
	9. Splitting 3	<ul style="list-style-type: none"> <li>Facilitates fluids flow &amp; stores buffer salt</li> </ul>
	10. Sensing	<ul style="list-style-type: none"> <li>L10: Captures the disease antibodies</li> </ul>
	11. Dock	<ul style="list-style-type: none"> <li>L11: Aligns sensing layer with other layers</li> </ul>
	12. Washing	<ul style="list-style-type: none"> <li>Protects the sensing layer from back-flow</li> </ul>
	13. Blotting	<ul style="list-style-type: none"> <li>Acts as a reservoir to wick-away excess fluids</li> </ul>
	14. Backing	<ul style="list-style-type: none"> <li>Protects the device and the user</li> </ul>

**Figure S13: An exploded-view schematic of the multiplex microfluidic paper-based analytical device used for the detection of anti-Brucella IgG and IgM antibodies in bovine serum. Layers 2-3, 5-9 and 12-13 are made of wax-patterned (green and blue colors) chromatography paper; layers 1 and 14 are made of cellulose acetate; layers 4 and 11 are made of double-sided tape; layer 10 is made of waxed-patterned (yellow color) nitrocellulose; and layer 12 is made of blotting layer.**






















Layer #	Group	Paper Pattern	Tape Pattern
1	A		
2	A		
3	B		
4	C		 
5	C		
6	D		
7	D		
8	D		
9	D		 REMOVE/PERM TAPE
10/11	E		 

Figure S14: Schematic of the groups of layers of patterned tape and paper.

### 1.2.2. Proof-of-concept device of indirect immunoassay for brucellosis using polymerization-based amplification (PBA) as a detection method

#### *Conjugation of Photoinitiator to Detection Antibody for Brucella Detection in Blood Serum*

We successfully conjugated eosin (M1074, Marker Gene Technologies, Inc.) onto bovine IgG (I5506, Sigma Aldrich) for use as a detection antibody using isothiocyanated eosin.

Approximately six eosin molecules per antibody achieved an acceptable balance of signal and solubility.

#### *Thymolphthalein-based Visualization of Positive Test Spots*

The amplification solution used for thymolphthalein-based PBA readout (Figure 3a) consisted of 150 mM triethanolamine (TEA), 400 mM (poly)ethyleneglycol diacrylate (PEGDA) ( $M_n=575$ ), 100 mM 1-vinyl-2-pyrrolidinone (VP), 0.9 mM thymolphthalein, 0.5  $\mu$ M free eosin, 20 mM hydrochloric acid (HCl) and 20 v/v% ethanol.

## 1.3. Results

### 1.3.1. Proof-of-concept studies of indirect immunoassays for the detection of brucellosis

We first developed an indirect immunoassay for the detection of brucellosis using IgG as an indicator of late-stage infection by this zoonotic pathogen. We then translated this detection chemistry for anti-*Brucella* bovine IgG from whole blood using PBA on a paper-based microfluidic device. We tested these devices using spiked bovine serum. Figure SI5a shows proof-of-concept results with 0.10 mg/mL eosin-conjugated bovine IgG spiked into 1:10 diluted bovine serum, procured and screened as courtesy from USDA.

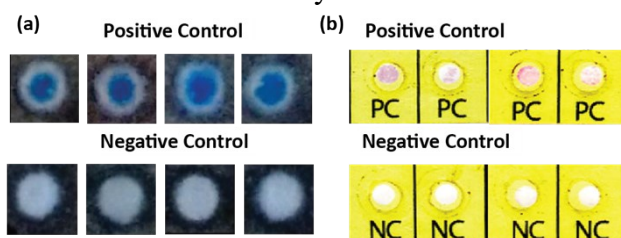


**Figure SI5. Proof-of-concept results for indirect immunoassays on paper-based devices. (a) Four replicates of 0.10 mg/mL eosin-conjugated bovine IgG spiked into diluted serum, and corresponding negative control experiments. (b) Four replicates of 0.45 mg/mL bovine IgG spiked into diluted serum, and corresponding negative control experiments.**

We also designed, optimized and batch-manufactured a paper-based device for duplex detection using gold nanoparticles for visual readout of results. The device comprised of 14 separate layers of wax-patterned chromatography paper, pressure-sensitive adhesive, nitrocellulose and blotting paper. Schematics of the device, with details on each layer of the device, and their function are shown in Figure SI6. We finally tested our devices using spiked bovine serum with commercially-available IgG. Figure SI5a shows proof-of-concept results with 0.45 mg/mL bovine IgG spiked into 1:10 diluted bovine serum, procured and screened as courtesy from USDA.

## 2. Proof-of-concept studies of indirect, multiplexed immunoassays for the detection of HIV and other STDs

### 2.1. Experimental Design

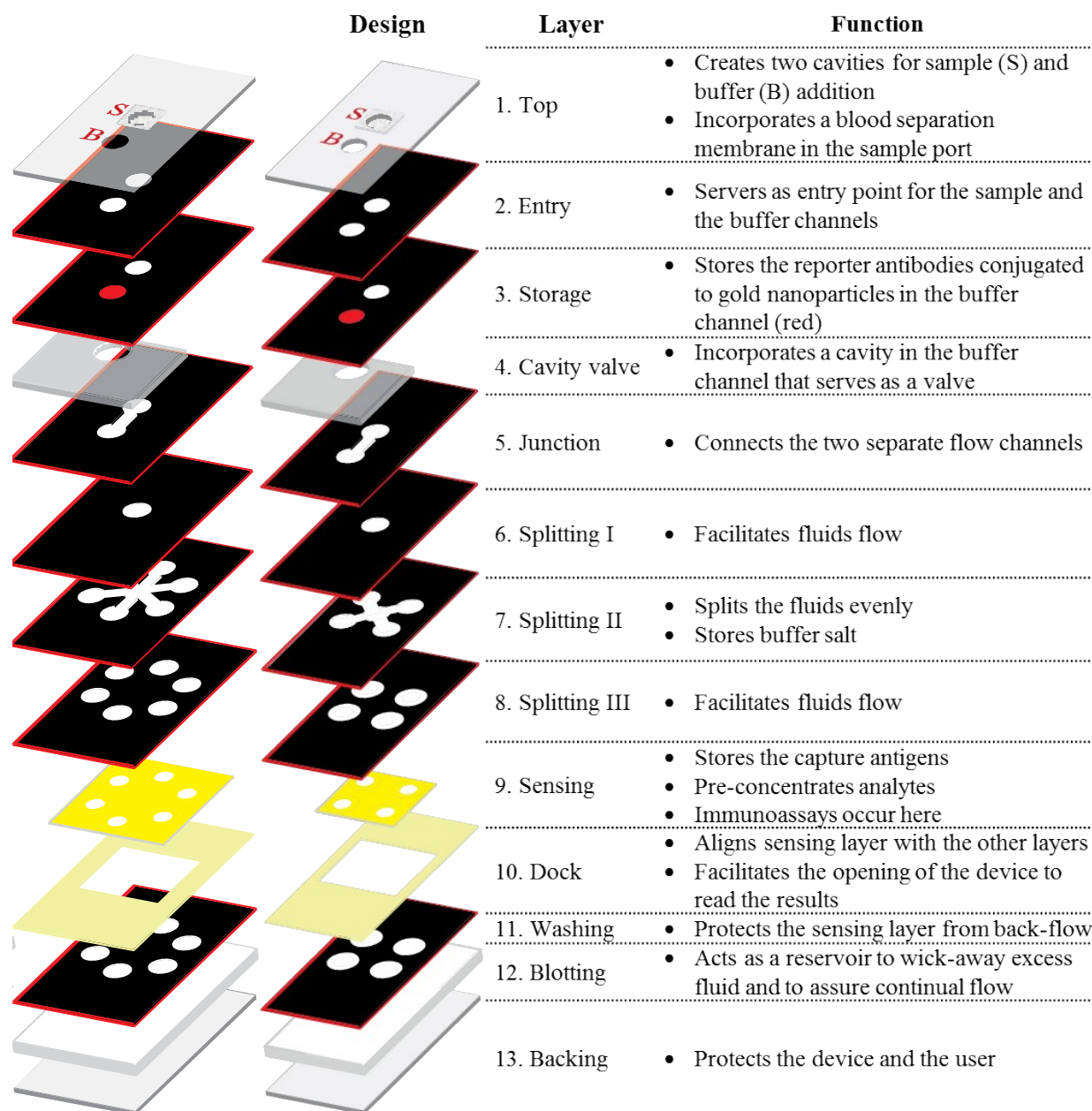
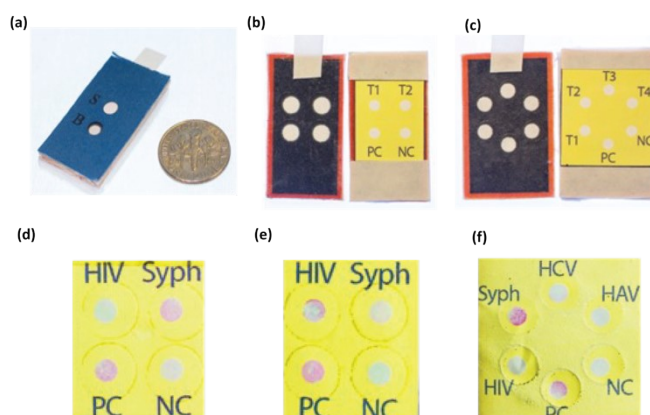


Figure S16. An exploded-view schematic, indicating layers and their specific function in duplex and quadruplex paper-based devices. Layers 1 and 13 were made of printing paper; layers 2-3, 5-8, and 11 are made of chromatography paper; layers 4 and 10 are made of three layers of double side adhesive; layer 9 is made of nitrocellulose; and layer 12 is made of blotting paper.



### 2.1.1. Results

We designed and fabricated modular devices, comprising of 13 separate layers for duplex and quadruplex detection from a single serum sample. Similarly to the previous examples, visual readout of results was performed by agglutination of gold nanoparticles. The key design difference here is that the device (Figure SI7) must be “opened” for visual readout by means of pulling a small tab, illustrated in Figures SI7b and SI7c. Schematics of the device, with details on each layer of the device, and their function are shown in Figures SI8. We tested these devices using commercially-available, human-serum-based standards for quality control. Qualitative, proof-of-concept results are shown in Figures SI7b to f. We successfully detected host antibodies against HIV virus (anti-HIV) and *Treponema pallidum* (anti-*Treponema pallidum*).



**Figure SI7. Proof-of-concept results for indirect immunoassays on duplex and quadruplex paper-based devices. (a) Photograph of closed device with dimensions of 17 mm by 20 mm by 50 mm (thickness, width, length). (b) Generic design for duplex device opened on the lay for visual readout. (c) Generic design for quadruplex device designed opened on the layer for visual readout. (d)(e) and (f) Qualitative results using VIROTROL® standards, intended to be representative of clinical positive samples. Labels on the devices denote sensing areas with immobilized capture antigens for the detection of the following: HIV for anti-HIV antibodies, Syph for anti-*Treponema pallidum*, HCV for anti-Hepatitis C virus, and HAV for anti-Hepatitis A virus. (d) Positive, serum-based reactive control VIROTROL® Syphilis LR-A for Syphilis. (e) Positive, serum-based reactive control VIROTROL® IV-2 for HIV. (f) Positive, serum-based reactive control VIROTROL® Syphilis LR-A for Syphilis.**

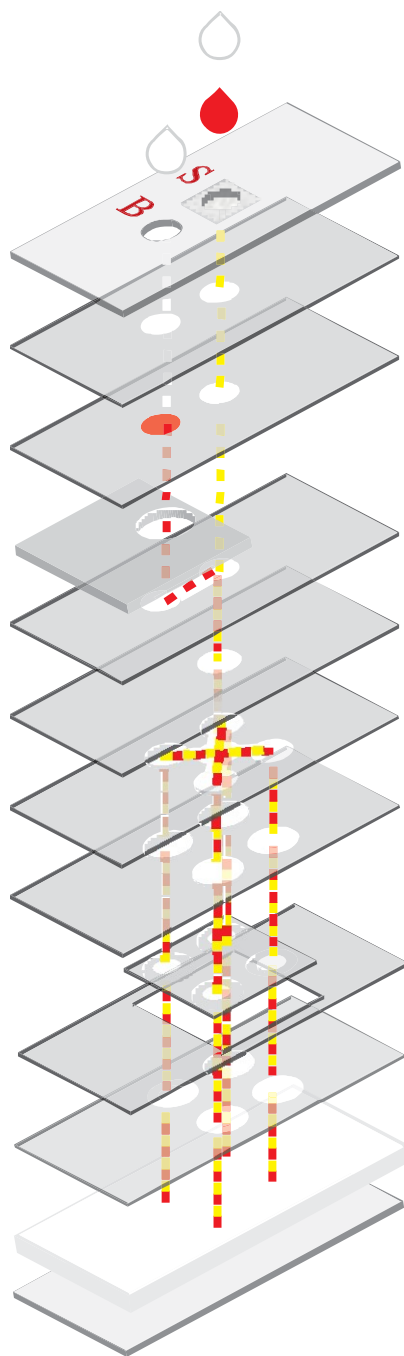


**Figure S8.** Flow paths in the duplex paper-based device. The red drop denotes a serum sample, which is then chased by an equal volume of saline buffer (white drop).

### 3. References

- 1 M. A. Geresu and G. M. Kassa, , DOI:10.4172/2157-7579.1000323.
- 2 B. Suo, J. He, C. Wu and D. Wang, *Bull. Exp. Biol. Med.*, 2021, **172**, 223–227.
- 3 United States. Animal and Plant Health Inspection Service, *Brucellosis in Cervidae: Uniform Methods and Rules, Effective September 30, 2003*, U.S. Department of Agriculture, Animal and Plant Health Inspection Service, 2003.
- 4 A. B. Ekiri, C. Kilonzo, B. H. Bird, E. VanWormer, D. J. Wolking, W. A. Smith, H. Masanja, R. R. Kazwala and J. A. K. Mazet, *J. Trop. Med.*, 2020, **2020**, 6586182.
- 5 J. D. Ruiz-Mesa, J. Sánchez-Gonzalez, J. M. Reguera, L. Martín, S. Lopez-Palmero and J. D. Colmenero, *Clin. Microbiol. Infect.*, 2005, **11**, 221–225.
- 6 A. S. Lukambagire, Â. J. Mendes, R. F. Bodenham, J. A. McGiven, N. A. Mkenda, C. Mathew, M. P. Rubach, P. Sakasaka, D. D. Shayo, V. P. Maro, G. M. Shirima, K. M. Thomas, C. J. Kasanga, R. R. Kazwala, J. E. B. Halliday and B. T. Mmbaga, *Sci. Rep.*, 2021, **11**, 5480.
- 7 R. Díaz, A. Casanova, J. Ariza and I. Moriyón, *PLoS Negl. Trop. Dis.*, 2011, **5**, e950.
- 8 S. Kim and H. D. Sikes, *Polym. Chem.*, 2020, **11**, 1424–1444.
- 9 K. Kaastrup and H. D. Sikes, *Chem. Soc. Rev.*, 2016, **45**, 532–545.
- 10 S. Kim, A. Martínez Dibildox, A. Aguirre-Soto and H. D. Sikes, *J. Am. Chem. Soc.*, 2021, **143**, 11544–11553.
- 11 M. S. Verma, M.-N. Tsaloglou, T. Sisley, D. Christodouleas, A. Chen, J. Milette and G. M. Whitesides, *Biosens. Bioelectron.*, 2018, **99**, 77–84.
- 12 A. K. Badu-Tawiah, S. Lathwal, K. Kaastrup, M. Al-Sayah, D. C. Christodouleas, B. S. Smith, G. M. Whitesides and H. D. Sikes, *Lab Chip*, 2015, **15**, 655–659.
- 13 K. Kaastrup and H. D. Sikes, *Lab Chip*, 2012, **12**, 4055–4058.
- 14 K. Kaastrup and H. D. Sikes, *RSC Adv.*, 2015, **5**, 15652–15659.
- 15 K. Kaastrup, L. Chan and H. D. Sikes, *Anal. Chem.*, 2013, **85**, 8055–8060.
- 16 M.-N. Tsaloglou, A. Nemiroski, G. Camci-Unal, D. C. Christodouleas, L. P. Murray, J. T. Connelly and G. M. Whitesides, *Anal. Biochem.*, 2018, **543**, 116–121.
- 17 J. T. Connelly, J. P. Rolland and G. M. Whitesides, *Anal. Chem.*, 2015, **87**, 7595–7601.